Carbon nanotube/graphene nanocomposite as efficient counter electrodes in dye-sensitized solar cells

Josef Velten
University Of Texas At Dallas

Attila J. Mozer
University of Wollongong, attila@uow.edu.au

Dan Li
University of Wollongong, danli@uow.edu.au

David Officer
University of Wollongong, davido@uow.edu.au

G G. Wallace
University of Wollongong, gwallace@uow.edu.au

See next page for additional authors

Recommended Citation

Authors

Josef Velten, Attila J. Mozer, Dan Li, David Officer, G G. Wallace, Ray Baughman, and A Zakhidov

Carbon nanotube/graphene nanocomposite as efficient counter electrodes in dye-sensitized solar cells

Josef Velten[1], Attila J Mozer[2], Dan Li[2], David Officer[2], Gordon Wallace[2], Ray Baughman[1] and Anvar Zakhidov[1]

[1] Alan G MacDiarmid Nanotech Institute, University of Texas at Dallas, Richardson, TX 75080-3021, USA
[2] ARC Centre of Excellence for Electromaterials Science, Intelligent Polymer Research Institute, University of Wollongong, NSW 2522, Australia

Abstract

We demonstrated the replacement of the Pt catalyst normally used in the counter electrode of a dye-sensitized solar cell (DSSC) by a nanocomposite of dry spun carbon multi-walled nanotube (MWNT) sheets with graphene flakes (Gr-F). The effectiveness of this counter electrode on the reduction of the triiodide in the iodide/triiodide redox (I^-/I_3^-) redox reaction was studied in parallel with the use of the dry spun carbon MWNT sheets alone and graphene flakes used independent of each other. This nanocomposite deposited onto fluorinated tin-oxide-coated glass showed improved catalytic behavior and power conversion efficiency (7.55%) beyond the use of the MWNTs alone (6.62%) or graphene alone (4.65%) for the triiodide reduction reaction in DSSC. We also compare the use of the carbon MWNT/Gr-F composite counter electrode with a DSSC using the standard Pt counter electrode (8.8%). The details of increased performance of graphene/MWNT composite electrodes as studied are discussed in terms of increased catalytic activity permitted by sharp atomic edges that arise from the structure of graphene flakes or the defect sites in the carbon MWNT and increased electrical conductivity between the carbon MWNT bundles by the graphene flakes.

(Some figures may appear in colour only in the online journal)

1. Introduction

Dye-sensitized solar cells (DSSC) have been demonstrated to be a viable, low cost method of producing solar electricity by use of a mesoporous layer of a semiconducting charge collector with a sensitizing dye, a redox mediator of I^-/I_3^- and a Pt catalyst to complete the redox reaction [1], of which a structural schematic of a standard and our carbon MWNT/graphene composite device is shown in figure 1. The highest performing DSSCs of these types can reach power conversion efficiencies of over 11% [2]. This is achieved by depositing platinum on a transparent conductive oxide (TCO) substrate. There exists a drawback with using Pt in any low cost application due to its scarcity as a precious metal. This has led to efforts to find suitable replacements for the Pt catalyst in DSSC with low cost materials, including the

use of carbon black, hard carbon spherules, polymer counter electrodes, nanocarbon, electrospun carbon and composites of conducting polymer/Pt or conducting polymer/carbon [3–13]. In an ideal situation, a single material may take the place of both TCO and the platinum catalyst, depending on the properties of the material itself. For carbon-based materials, a good catalyst needs to have sharp atomic edges exposed to the electrolyte in the DSSC. In carbon nanotubes, this is usually achieved at defect sites where dangling bonds are exposed to the electrolyte, which can be found during formation or induced in a simple post-processing, such as an O_3 treatment [14]. This need for a good catalyst also needs to be balanced against having good structural integrity for the carbon nanotubes to be good conductors, as too many defects in the structure will harm the conductivity of the nanotubes. In general, these properties need to be
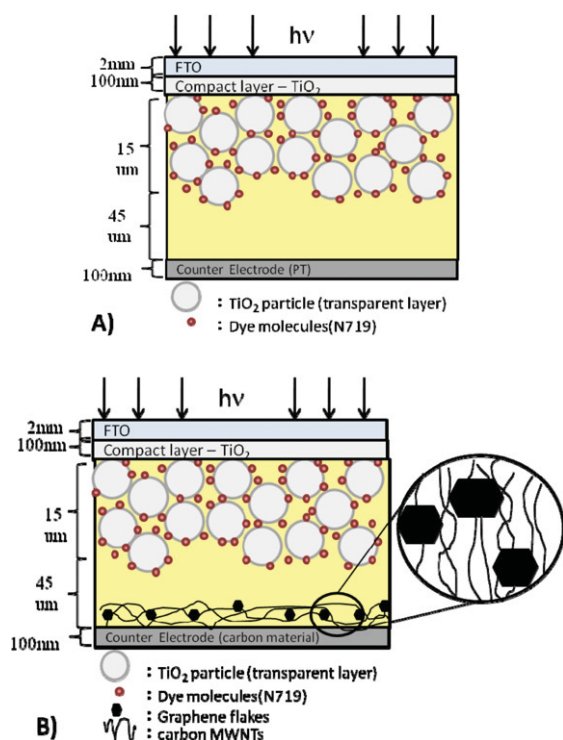
Figure 1. (a) Schematic of a dye-sensitized solar cell.
(b) Schematic of a dye-sensitized solar cell with a carbon
MWNT/graphene composite. The expansion of the counter
electrode portion of the scheme is to show the placement of the
graphene to act as a conducting bridge and as a space to offer the
sharp atomic edges for catalysis.

balanced against each other, in order to create a good catalyst
and conductive substrate. This paper describes an alternative
solution to the balancing issue, using dry spun multi-wall
carbon nanotubes [15] and exfoliated graphene from aqueous
solution [16]. The highly catalytic graphene is functionalized
onto the carbon MWNTs to support the reduction of the I_3^-
in the redox couple that mediates the charge between the two
electrodes of the DSSC. We show that using both the graphene
and the carbon MWNT in a functional network is necessary
to obtain DSSC performance comparable to the Pt-coated
standard counter electrode.

Carbon nanotubes have previously been used as a counter
electrode in DSSCs [17–19] where they have been tested
to give high power conversion efficiencies. The carbon
nanotubes that show results that are closest to Pt are usually
single-walled carbon nanotubes (carbon SWNTs), with the
carbon MWNTs showing lower overall power conversion
efficiency when compared to carbon SWNTs. While there
is a clear advantage to using carbon SWNTs in the counter
electrodes of DSSCs, there is greater development in the
method of mass production of carbon MWNTs, which makes
it valuable to investigate methods to improve the reductive
properties of carbon MWNTs in the I^-/I_3^- redox couple in
the DSSCs.

Graphene films have been used as the DSSC counter
electrode for more than just a catalyst material [12, 20–22]. It
has also been used as an optically transparent replacement for
the more traditional transparent conductive oxides of indium

tin oxide (ITO) and fluorinated tin oxide (FTO). There have
been demonstrations of a graphene substrate replacing ITO
for a solid state DSSC with a power conversion efficiency of
0.84% and a transparency 70.7% at 1000 nm wavelength [23].
Being an ordered carbon, it also suggests itself as a possible
candidate for use as a catalyst in the counter electrode of
the DSSC. In general electrochemical characterization tests
of carbon materials, it has been demonstrated that catalysis
has been performed at defect sites and atomic edges [24], so
if graphene can be organized to present sharp atomic edges
then a high rate of reduction can be achieved with a small
amount of material. However, using pure graphene is not
conducive to a good device, as most deposition techniques
will result in smooth surfaces of graphene on the DSSC which
does not allow for a high surface area of interaction between
the redox couple and the graphene's atomic edges in the
catalytic component of the graphene, which has been noted
to be critical in the operation of a DSC using carbon-based
catalysts [7].

There also has been a recent report on the usage of
graphene and carbon MWNTs used in conjunction. In that
report, graphene has been used to keep carbon MWNTs
aligned in a transfer process from a substrate of SiO_2 to
an FTO substrate used in the DSSC, primarily using the
graphene as a binder to keep the carbon MWNTs aligned
with respect to each other, rather than to use graphene for
participation in the reduction of triiodide to iodide [20]. The
work presented in this paper took a different approach, using
carbon MWNTs that were aligned from a dry spinning process
and using the carbon MWNTs to be a mechanical support
structure for the graphene participant in the reduction of the
triiodide used in the DSSC, and to provide a lower overall
sheet resistance of the counter electrode by connecting the
bundles of carbon MWNTs with the graphene flakes, rather
than using the graphene as a support structure for transferring
vertically aligned carbon MWNTs.

2. Experimental set-up

Glass with a fluorinated tin oxide surface layer (SnO_2:F, FTO
glass, 8 Ω/square, Hartford Glass) was cut and sonicated in
a successive series of baths of DI water, ethanol, acetone
and toluene for 15 min each and then set under a UV lamp
for 15 min to clean the surface. After cleaning they were
immersed in a bath of 40 mM solution of aqueous $TiCl_4$
for 30 min at 70 °C and then removed and rinsed with DI
water which helps with adhesion of the TiO_2 layer to the
substrate [25]. The TiO_2 active layer (Dyesol NR-18) was
then doctor-bladed onto the FTO plate surface to a thickness
of approximately 10 μm, dried at 100 °C for 15 min and
then a second layer (Dyesol WER-O4) was doctor-bladed
on top of the transparent, active layer, and dried again at
100 °C for 10 min. This bilayer of paste was then sintered
for 30 min at 500 °C. After this first sintering operation
the FTO plates were then immersed in a new 40 mM
solution of aqueous $TiCl_4$ at 70 °C for 30 min, cleaned in
DI water, and sintered a second time at 500 °C for 30 min.
These plates were then cooled to 80 °C immersed in a 1:1

Table 1. Comparison of DSC cell performance.

Counter electrode	U_{oc} (V)	I_{sc} (mA cm^{-2})	FF	(%)	$R/\square$ (Ω)	Counter electrode j_0 (mA cm^{-2})
MWCNT	0.74	15.54	0.576	6.62	30	6.0
MWCNT and graphene	0.75	16.05	0.627	7.55	15	18.4
PT reference	0.79	16.27	0.688	8.8	n/a	15.5
Graphene	0.75	13.09	0.473	4.64	94	1.29

ratio of acetonitrile and tert-butanol with 2.52×10^{-4} M of *cis*-diisothiocyanato-bis(2,2′-bipyridyl-4,4′-dicarboxylato) ruthenium(II) bis(tetrabutylammonium) in solution, known as N719 dye.

The counter electrode FTO plate had a small hole drilled into it and was cleaned in the same manner as the working electrode above. When the FTO plate has been cleaned then dry spun multi-walled carbon nanotube sheets were added as made through a technique similar to what was discussed in another paper [15]. Iron-coated silicon substrates are inserted into a 3″ quartz tube furnace and cleaned by vacuum purging the tube three times and flowing helium to provide an inert atmosphere. The furnace is heated to a growth temperature of 750 °C. Once the system is at the correct temperature a carbon source gas of acetylene is injected into the furnace along with hydrogen to provide growth enhancement. After 6–12 min of growth time the acetylene and hydrogen is stopped and the system is cooled to ambient. The substrates collected are immediately ready for sheet pulling.

Solution processable graphene was made using a process involving the method developed by Li *et al* [16]. The solution was prepared by taking natural graphite and exfoliating it into graphite oxide by a modified Hummers method. From there, the graphite oxide was suspended in an aqueous solution where it was subjected to dialysis to remove excess salts and acids. This graphite oxide was then converted to graphene oxide by ultrasonication and a solution of hydrazine and ammonia was introduced into the solution to make graphene from the reduction of graphene oxide.

The carbon MWNT sheets were dry spun and deposited onto the surface of an FTO plate one layer at a time, then densified with ethanol. Then a 0.075 ml drop of the graphene solution was drop-cast onto the carbon nanotube sheets and the solution was evaporated at 80 °C. These last two steps were repeated until five layers of MWCNTs and 0.375 ml of graphene solution were deposited onto the FTO plate. After the final addition of graphene solution, the counter electrode was sintered at 250 °C for 10 min to remove any oxygen functionalized on the graphene and carbon nanotubes [26]. Reference counter electrodes composed of five layers of MWCNT sheets, drop-castings of 0.375 ml of graphene solution and thermally decomposed Pt counter electrodes were also used for comparison. The two plates were sandwiched together with a 60 μm Surlyn® gasket and then hot pressed to form a seal. The electrolyte used in this test was composed of 1-methyl-3-propylimidazolium iodide (0.6 M), iodine (0.03 M), guanidine thiocyanate (0.1 M) and 4-tert-butylpyridine (0.5 M) in acetonitrile. The cells were then masked and tested on a Thermo Oriel solar
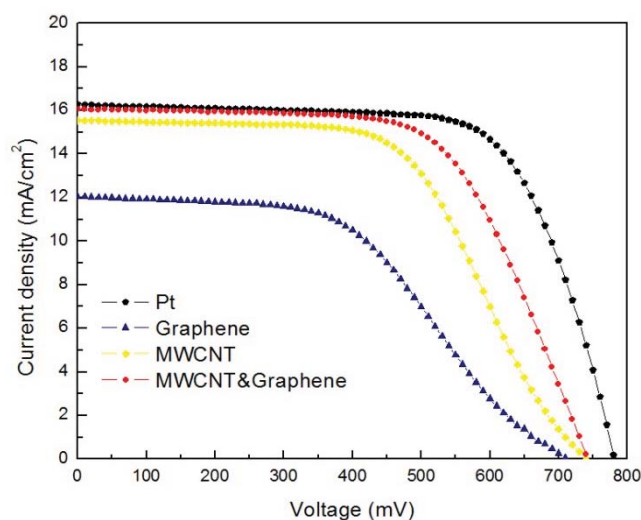
Figure 2. Comparison of DSC cells with MWCNTs, MWCNTs and graphene, and Pt reference cell.

simulator set at A.M. 1.5 G radiation with the intensity set at 100 mW cm^{-2}. Impedance measurements were taken under operating conditions (solar stimulation) under zero applied bias over the range of 10^6–10^{-2} Hz range with a 10 mV ac amplitude using a PGZ 301 potentiostat/galvanostat/EIS.

Sheet resistances of the counter electrode materials were also measured by depositing the counter electrode materials on glass slides with contacts made by silver paste. The intention of this procedure was to help in determining the serial resistive losses of the counter electrode material.

3. Results and discussion

The addition of graphene to the MWCNT sheets yielded a respectable increase over using the MWCNT sheets alone in the DSSC. Figure 2 is a comparison of the *I–V* curves with different counter electrodes, with table 1 giving a summary of the data in figure 2. Deposition of graphene onto the carbon MWNTs is confirmed by SEM micrographs in figure 4. The composite shows the greatest improvement is in the fill factor (62.7%) compared to using graphene alone (47.3%) or the dry spun carbon MWNTs (57.6%). To properly interpret why this is so, we must take a look at the electrochemical impedance of the solar cells, which is shown in figure 3. Modeling of the DSSCs equivalent circuit arises from the method discussed in [27] for the carbon MWNTs, the composite MWNT/graphene and the Pt counter electrode, while the graphene counter electrode DSSC was better described by a separate model, both of which are shown in figure 5. The R_{ct}
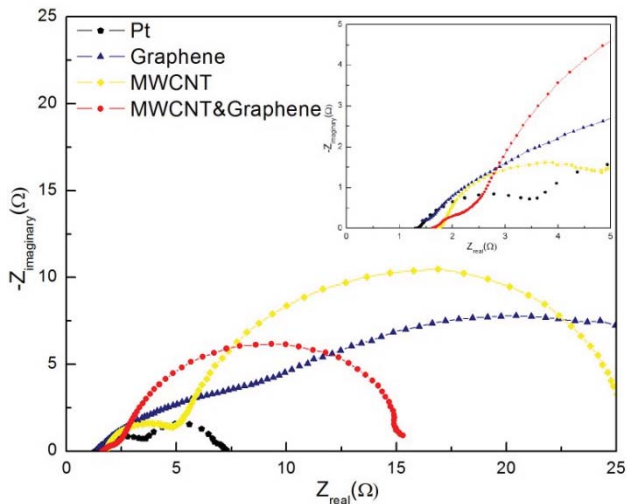
Figure 3. Nyquist plot of the MWCNT sheet counter electrode and the composite MWCNTs and graphene counter electrode with Pt reference.

of the counter electrode is determined by the first semicircle of the impedance graph which means that the R_{ct} of the counter electrode of the devices show yield values of 20, 4.3, 1.4 and 1.7 Ω for graphene, carbon MWNTs, composite MWNTs/graphene and platinum reference cell, respectively. The use of graphene alone does not fit the model well with the experiment in the standard equivalent circuit, but is more amenable to a different modeling set-up that is outlined in [5], which was used for modeling DSSCs using carbon black, specifically for ones that had insufficient thickness, and consequently surface area for chemical reduction, for high performance. From the values of R_{ct}, we can give estimates of the exchange current density j_o at the counter electrode. The exchange current density of an electrode (j_0) and R_{ct} have a relationship as shown in equation (1):

$$j_0 = \frac{RT}{nFR_{ct}} \qquad (1)$$

where R is the universal gas constant, T is the absolute temperature, F is the Faraday constant and n is the stoichiometric number of electrons involved in a reaction. In a practical concern, for a good exchange current density in a DSSC counter electrode, a significantly higher exchange current density above the photoelectrode's produced current density is desirable. For each of the counter electrodes, table 1 gives a summary of the exchange current densities involved. The EIS of the composite of carbon MWNTs and graphene shows an explanation as to why there is an increased fill factor over the use of carbon MWNTs or graphene alone. The lower R_{ct} means there are fewer losses at the electrolyte/counter electrode interface, giving a better operation for the cell, but still having a number of losses through the diffusion resistance through the cell, giving a lower performance than the Pt reference cell. The second semicircle, corresponding to the TiO$_2$/dye interface with electrolyte, is smaller than the one seen in the MWNTs. The carbon MWNTs cannot reduce the I_3^- as quickly as it can be generated at the working electrode, as reduction takes place at the sharp atomic edges of carbon materials. For carbon-based counter electrodes, such as carbon MWNTs, the reduction takes place at the defect sites and the carbon MWNTs do not have enough of these defect sites to keep up with the production of I_3^- at the photoanode. This would then build up to a steady state where there is more I_3^- at the TiO$_2$/dye and electrolyte interface, which would show up on an EIS test as a larger capacitance than what one would see using a Pt counter electrode. This buildup of charge would also have an effect on the V_{oc} of the DSSC by having more I_3^- at the interface, i.e. there would be more recombination of charge which would lower the electron density in the TiO$_2$ and give a lower yield of both current and a lower open circuit voltage, which is what we see when we compare carbon MWNTs to the Pt reference. The
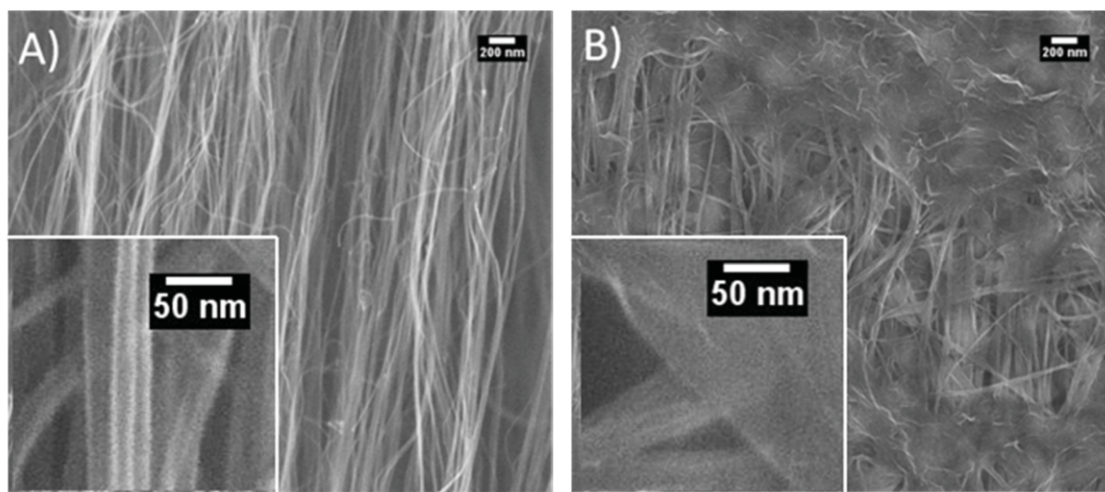

Figure 4. (a) SEM picture of MWCNT sheet without graphene and (b) with the addition of graphene: the increase in surface area allows for more reduction of the redox reaction. Inset of (b) shows a close-up of graphene connecting two bundles of carbon MWNTs creating a bridge across the two.
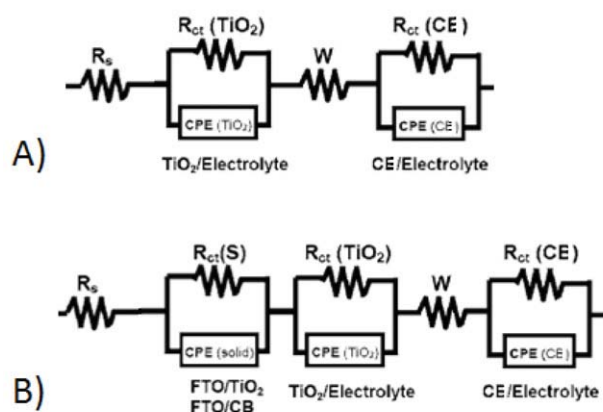
Figure 5. (a) Simulation of equivalent circuit for standard DSSCs, where there is a capacitive and resistive element at the TiO₂/electrolyte interface and at the counter electrode, with a series and Warburg impedance. (b) Simulation of equivalent circuits used for graphitic counter electrode materials. For this paper, we found that graphene only fits the model of (b) while the MWCNTs and MWCNTs/graphene made good fits to both models.

poor performance of the Gr-F graphene alone has a similar explanation as well. Without the carbon MWNTs to provide a structure for the graphene, they formed smooth layers on top of one another, limiting the total surface area as in the case for optimization tests for carbon black counter electrodes. When we took the sheet resistance of each of the counter electrode materials on a glass substrate we can lend even more weight to this reasoning. In the sheet resistance measurements on glass substrates, the sheet resistance of the graphene was $R_{sh} = 94 \ \Omega/\text{square}$. When compared to the five layers of carbon MWNTs ($R_{sh} = 30 \ \Omega/\text{square}$) or the composite of MWNTs and Gr-F ($R_{sh} = 15 \ \Omega/\text{square}$) Gr-F alone showed a much higher resistance than the other materials tested. This high serial resistance and low available surface area of the graphene paints a clear picture as to why the graphene alone is not a good counter electrode material. The Gr-F alone *e* is unable to avoid high serial resistive losses when acting as the counter electrode material, and the graphene alone is also incapable of keeping up with the I_3^- generation of a standard DSSC. The serial resistive losses from the motion of the electrons through the carbon MWNTs to the substrate give a lower fill factor than that of the platinum counter electrode, even though the R_{ct} of the platinum was higher. Platinum, being of the order of a few nanometers thick, has negligible resistive losses to the FTO substrate when compared to any of the carbon materials.

Therefore only the composite of MWCNT/Gr-F can solve the problem of having low enough charge transfer resistance R_{ct} (which is provided by the Gr-F component) and, at the same time, a low sheet resistance $R_{sh} < 15 \ \Omega/\text{square}$ (which is provided by the multiple layers of carbon MWNT sheets connecting graphene flakes). Such a functional composite is, in fact, an analog of the Pt/FTO composite counter electrode in which GRN plays the role of Pt for low R_{ct}, while MWNTs play the role of FTO for R_{sh}.

4. Conclusion

In this paper we demonstrated the necessity of using a composite of graphene and carbon MWNTs for the efficient reduction of I_3^- at the counter electrode, allowing us to develop a DSSC free of platinum that gives a power conversion efficiency of 7.55%, which shows a performance 86% as efficient as the Pt reference cell used in this study. The study of these cells supports the idea that, for efficient performance of a carbon-based counter electrode, there needs to be many sharp atomic edges exposed to the ions in the electrolyte for increased catalytic effect, i.e. low enough R_{ct}, which can be achieved through the use of depositing graphene onto sheets of carbon MWNTs. At the same time, the addition of graphene flakes provides the necessary R_{ct}, increasing the conductivity of the carbon MWNTs/Gr-F nanocomposite and decreasing sheet resistance and the cell's overall internal resistance.

References

[1] O'Regan B and Gratzel M 1991 A low-cost, high-efficiency solar cell based on dye-sensitized colloidal TiO₂ films *Nature* **353** 737–40

[2] Chiba Y *et al* 2006 Dye-sensitized solar cells with conversion efficiency of 11.1% *Japan. J. Appl. Phys.* **45** 638–40

[3] Saito Y *et al* 2004 I-/I3- redox reaction behavior on poly(3,4-ethylenedioxythiophene) counter electrode in dye-sensitized solar cells *J. Photochem. Photobiol.* A **164** 153–7

[4] Fan B *et al* 2008 Conducting polymer/carbon nanotube composite as counter electrode of dye-sensitized solar cells *Appl. Phys. Lett.* **93** 143103

[5] Murakami T N *et al* 2006 Highly efficient dye-sensitized solar cells based on carbon black counter electrodes *J. Electrochem. Soc.* **153** A2255–61

[6] Hong W *et al* 2008 Transparent graphene/PEDOT-PSS composite films as counter electrodes of dye-sensitized solar cells *Electrochem. Commun.* **10** 1555–8

[7] Imoto K *et al* 2003 High-performance carbon counter electrode for dye-sensitized solar cells *Sol. Energy Mater. Sol. Cells* **79** 459–69

[8] Huang Z *et al* 2007 Application of carbon materials as counter electrodes of dye-sensitized solar cells *Electrochem. Commun.* **9** 596–8

[9] Ramasamy E *et al* 2007 *Nanocarbon Counterelectrode for Dye Sensitized Solar Cells* vol 90 (New York: AIP)

[10] Joshi P *et al* 2010 Electrospun carbon nanofibers as low-cost counter electrode for dye-sensitized solar cells *ACS Appl. Mater. Interfaces* **2** 3572–7

[11] Xiaoguang M *et al* 2010 High-performance dye-sensitized solar cells with gel-coated binder-free carbon nanotube films as counter electrode *Nanotechnology* **21** 395202

[12] Hsieh C-T, Yang B-H and Lin J-Y 2011 One- and two-dimensional carbon nanomaterials as counter electrodes for dye-sensitized solar cells *Carbon* **49** 3092–7

[13] Veerappan G, Bojan K and Rhee S -W 2011 Sub-micrometer-sized graphite as a conducting and catalytic counter electrode for dye-sensitized solar cells *ACS Appl. Mater. Interfaces* **3** 857–62

[14] Trancik J E, Barton S C and Hone J 2008 Transparent and catalytic carbon nanotube films *Nano Lett.* **8** 982–7

[15] Zhang M *et al* 2005 Strong, transparent, multifunctional, carbon nanotube sheets *Science* **309** 1215–9

[16] Li D *et al* 2008 Processable aqueous dispersions of graphene nanosheets *Nature Nano* **3** 101–5

[17] Suzuki K *et al* 2003 Application of carbon nanotubes to counter electrodes of dye-sensitized solar cells *Chem. Lett.* **32** 28–9

[18] Nam J G *et al* 2010 Enhancement of the efficiency of dye-sensitized solar cell by utilizing carbon nanotube counter electrode *Scr. Mater.* **62** 148–50

[19] Han J *et al* 2010 Water-soluble polyelectrolyte-grafted multiwalled carbon nanotube thin films for efficient counter electrode of dye-sensitized solar cells *ACS Nano* **4** 3503–9

[20] Choi H *et al* 2011 Dye-sensitized solar cells using graphene-based carbon nano composite as counter electrode *Sol. Energy Mater. Sol. Cells* **95** 323–5

[21] Roy-Mayhew J D *et al* 2010 Functionalized graphene as a catalytic counter electrode in dye-sensitized solar cells *ACS Nano* **4** 6203–11

[22] Zhang D W *et al* 2010 Graphene nanosheet counter-electrodes for dye-sensitized solar cells *INEC2010: 3rd Int. Nanoelectronics Conf.*

[23] Wang X, Zhi L and Mullen K 2007 Transparent, conductive graphene electrodes for dye-sensitized solar cells *Nano Lett.* **8** 323–7

[24] Pumera M 2009 The electrochemistry of carbon nanotubes: fundamentals and applications *Chem.—Eur. J.* A **15** 4970–8

[25] Sommeling P M *et al* 2006 Influence of a TiC$_{l4}$ post-treatment on nanocrystalline TiO$_2$ films in dye-sensitized solar cells *J. Phys. Chem.* B **110** 19191–7

[26] Boehm H P 2002 Surface oxides on carbon and their analysis: a critical assessment *Carbon* **40** 145–9

[27] Han L *et al* 2004 Modeling of an equivalent circuit for dye-sensitized solar cells *Appl. Phys. Lett.* **84** 2433–5